

ARTICLE

## Efficacy and Safety of the Atrial Septal Defect Closure for Patients with Absent or Malaligned Aortic Rim Using a Figulla Flex II Device Flared and Straddling Behind the Aorta

Masataka Kitano<sup>1,2,\*</sup>, Kazuto Fujimoto<sup>1</sup>, Atsuko Kato<sup>1</sup>, Ken-ichi Kurosaki<sup>1</sup> and Isao Shiraishi<sup>1</sup>

<sup>1</sup>Department of Pediatric Cardiology, National Cerebral and Cardiovascular Center, Osaka, Japan

<sup>2</sup>Department of Pediatric Cardiology, Okinawa Prefectural Nanbu Medical Center & Children's Medical Center, Okinawa Prefecture, Japan

\*Corresponding Author: Masataka Kitano. Email: kitanokitano.masataka@yahoo.co.jp

Received: 07 December 2020 Accepted: 07 January 2021

### ABSTRACT

**Background:** Although transcatheter closure of atrial septal defect (ASD) is safe and effective for patients with sufficient rim, ASD patients with absent and/or malaligned aortic and/or superior rim have higher risks of device embolization and cardiac erosion. We have treated such high-risk patients using a Figulla Flex II (FFII) device shaped flared and straddling behind the aorta because this method would avoid such serious complications. However, its long-term efficacy and safety remain unclear. Therefore, the midterm efficacy and safety of this method were studied. **Methods:** We retrospectively evaluated the outcome of 47 consecutive patients with such rim (age 6–73 years, weight 17–75 kg, 31 females) treated with this method at our hospital between February 2016 and September 2019. To make the flared and straddling shape, we selected a FFII 4–6 mm larger than the balloon sizing diameter by stop-flow technique. We also studied the device shape, the disc pressure to the Valsalva wall and their changes over 6 months by transesophageal echocardiography. **Results:** All procedures were successful, and leakage disappeared within 1 year. During a mean follow up of  $37 \pm 12$  months, complications included a transient sinus node dysfunction and one I° atrioventricular block within 3 months. Whole device shape changed from bulky to thin: the device waist and thickness significantly decreased by around 1.5 mm and 3.5 mm, respectively ( $p < 0.05$ ), but the two discs remained flared and straddling behind the aorta over 6 months; therefore, the disc edges seldom pressed the Valsalva wall perpendicularly, even though the inner plane of either disc often slightly pressed the wall. **Conclusions:** ASD closure using a FFII shaped flared and straddling behind the aorta is probably effective and safe for patients with absent and/or malaligned aortic and/or superior rim although requiring care for conduction disorders.

### KEYWORDS

Atrial septal defect; catheter intervention; device embolization; cardiac erosion; conduction disorder

## 1 Introduction

Amplatzer septal occluder (ASO; St. Jude Medical, Plymouth, MN) is one of the most used devices for transcatheter closure of secundum atrial septal defects (ASDs). Its advantages are the lower rate of early complications and shorter duration of hospital stay compared with surgical closure [1]. However, serious



This work is licensed under a Creative Commons Attribution 4.0 International License, which permits unrestricted use, distribution, and reproduction in any medium, provided the original work is properly cited.

complications such as device embolization (0.62%) or cardiac erosion (0.27%) were reported [2]. Device embolization usually occurs in patients with undersized device placement and/or deficient rims [3]. Meanwhile, cardiac erosion usually occurs in patients with deficient/absent aortic and/or superior rim [4–6]. Although erosion is caused by many factors, mechanisms underlying its development are listed below. Firstly, the disc edge of an oversized device bruises the atrial and aortic walls like a saw [5]. In addition, the disc edge of an undersized device with motion relative to the aorta presses the atrial and aortic walls perpendicularly [6,7]. Furthermore, change in device shape behind the aorta from flared to close for several months causes the disc edge to press the atrial and aortic walls perpendicularly [6,8,9]. The risk of erosion becomes higher in patients with absent and/or malaligned aortic and/or superior rim, and/or on drugs such as steroid [10].

Occlutech<sup>®</sup> Figulla<sup>®</sup> Flex II device (FFII; Occlutech GmbH, Jena, Germany) is widely used in Europe and Asia recently. Since the left atrial disc has no hub and contains less metal in the center, FFII is more flexible and reduces the shear forces than ASO [11]. For this reason, cardiac erosion had not been reported after FFII placement until 2019 [12] although device embolization occurred more (1.5% at placement; 0.4% during follow up) compared to ASO [11,13]. However, seven cases developing erosion after Figulla Flex devices placement were reported in 2019 [14]. In one of them, who had a malaligned absent aortic rim developed a cardiac tamponade 4 days later after placement, the right disc edge was strongly pressing the Valsalva wall perpendicularly immediately after placement [13]. Thus, patients with absent and/or malaligned aortic and/or superior rim have a higher risk of device embolization as well as cardiac erosion.

From August 2005 to June 2016, we treated 908 patients using an ASO and 30 patients using a FFII, who had various types of ASD including absent and/or malaligned aortic and/or superior rim. We routinely performed 6-month-follow-up transesophageal echocardiography (TEE) for these high-risk patients to evaluate the device shape, the disc edge pressure to the Valsalva wall and those changes [6,15]. We found that a FFII larger than the balloon sizing diameter (BSD) shaped the two discs flared and straddling behind the aorta in patients with absent and/or malaligned aortic rim, and the disc edges seldom pressed the Valsalva wall perpendicularly. Thus, we felt that this shape would avoid device migration as well as erosion. Since then, we have intentionally treated such high-risk patients using a large-sized FFII flared and straddling behind the aorta to avoid these serious complications. Although we believe that this closure method is ideal for such high-risk patients, the long-term efficacy and safety remains unclear. Therefore, we studied a midterm efficacy and safety of this method for such patients, including change in device shape over time.

## 2 Methods

### 2.1 Study Population

The research ethics committee of National Cerebral and Cardiovascular Centre approved this retrospective study with an opt-out method (R20015). We reviewed the catheter intervention registry of our Department. There were 165 patients who had ASD closure performed using a FFII from February 2016 to September 2019. Among these patients, we tried this ASD closure method in 47 consecutive patients who had an absent or extremely deficient, the latter defined as a rim length of  $\leq 1$  mm in a wide area, aortic and/or superior rim with or without rim malalignment. We therefore included the 47 cases as study population.

### 2.2 Device Selection to Shape Flared and Straddling behind the Aorta

Usually, we selected a FFII with a 4 mm–6 mm larger than the BSD by stop-flow technique for such high-risk patients. We preferred a FFII approximately 4 mm larger than the BSD in patients weighing around 20 kg, for example 24 mm device for the BSD 19.5 mm and 19.5 mm device for the BSD 16.0 mm, while selecting a 6 mm larger than that in patients weighing more than 30 kg, for example

30 mm device for the BSD 23 mm (Fig. 1). However, especially in small children weighing around 20 kg with a short atrial septal length (ASL), we first selected the largest device whose diameter plus rim length of the left atrial disc was within the ASL plus 2 mm to avoid conduction disorders. We measured the ASL on a TEE plane including a short axis of the aorta and the center of the balloon during the balloon inflation (Fig. 2). This is because this selection is thought to form the two discs flared and straddling behind the aorta in short ASL. If the device shape did not flare and straddle over the aorta enough and either disc edge pressed the Valsalva wall perpendicularly to deform it deeply, we exchanged the device to 3 mm larger one.

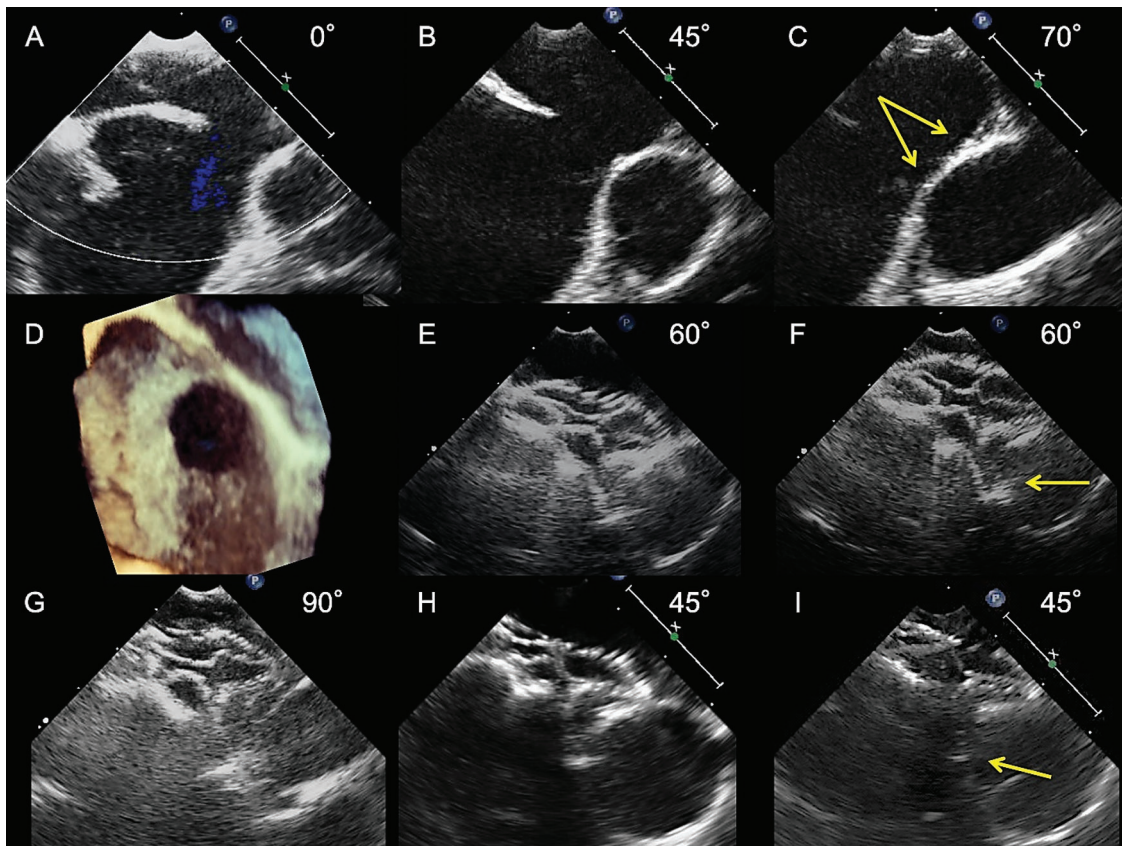


**Figure 1:** Transesophageal echocardiograms showing the process of selecting an FFII to shape the two discs flared and straddling behind the aorta. An 8-year-old boy weighing 21 kg had a 13.9 mm × 11.5 mm ASD with a 0.5 mm-length aortic rim in a wide area only (A, B, D) and a malaligned no superior rim (C, arrows, and D). A 21 mm FFII was placed into the ASD for a BSD of 16.6 mm. Immediately after placement (E, the farthest phase of the device from the Valsalva; F, the nearest phase of the device), two discs were flared and straddling over the Valsalva (E, F) and the superior side (G). The device looks flexible and bulky, and not the edge but the inner plane of the right atrial disc is slightly pressing the Valsalva wall intermittently (F, arrow). At 6 months after placement (H: Farthest phase, I: Nearest phase), the device shape becomes compact, but the two discs are kept flared and straddling behind the aorta; hence, the right atrial disc inner plane is slightly pressing the Valsalva wall intermittently (I, arrow)

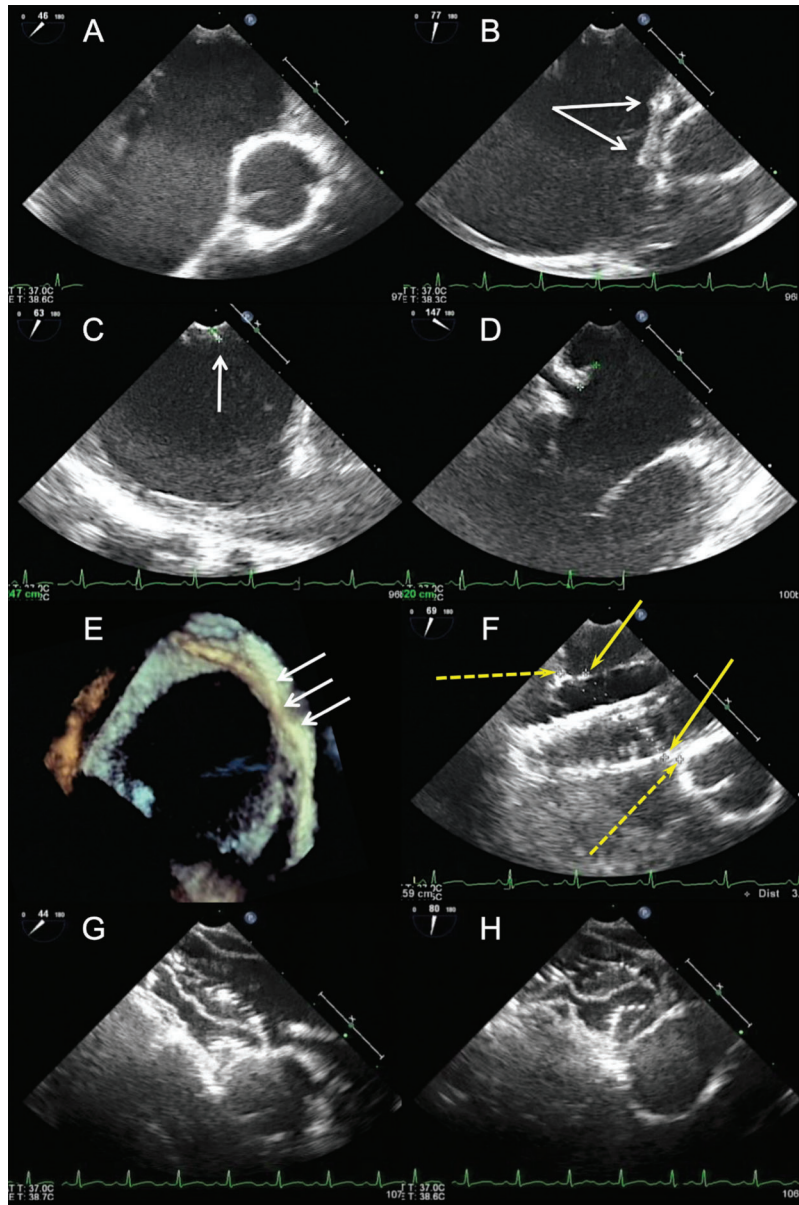


**Figure 2:** Transesophageal echocardiograms showing the selection of a device in small children with short ASL. A 7-year-old girl weighing 19 kg had a 23.5 mm × 19.5 mm ASD with absent aortic rim (A and E, arrows), malaligned superior rim (B, arrows), and 2.5 mm deficient inferior vena cava rim (C, arrow). Coronary sinus rim length was 5.7 mm (D). BSD by the stop-flow technique was 25.5 mm (F, between continuous line arrows). A 27 mm FFII, not 30 mm, was selected because the ASL behind the Valsalva was only 33 mm (F, between dashed line arrows). After placement, the two discs were flared and straddling over the Valsalva (G) and the superior side (H). Device selection in a case with short ASL is as follows: The largest device which diameter + rim length of left trial disc  $\leq$  ASL + 2 mm

### 2.3 Data Collection and Measurement

From the medical records of the 47 patients, we collected the baseline characteristics including age, sex, height, weight, body surface area, Qp/Qs and device size at the placement. By TEE before placement, we

collected the maximum ASD diameter, each minimum rim length (aortic, superior, superior vena cava, posterior, inferior vena cava, coronary sinus and mitral valve), absent aortic rim in multiple views, absent aortic rim at  $0^\circ$  plane (which is called bald aorta) [10] and malaligned aortic/superior rim, BSD by stop-flow technique, and ASL on a plane containing a short axis of the aorta and the center of the balloon during the balloon inflation. We defined a rim with the minimum length less than 5 mm as deficient one. In addition, we collected presence/degree of residual leakage by TEE at 6 months and by transthoracic echocardiography (TTE) one year after placement. We used the degree of residual leakage with width of color Doppler as with a previous study: small  $\leq 2$  mm < moderate < 4 mm  $\leq$  large [16]. By performing TEE immediately and 6 months after placement, we evaluated the device shape and presence of Valsalva wall deformation pressed by the discs. we measured the waist diameter and maximum device thicknesses at the center, Valsalva side and opposite side on lines perpendicular to the line containing the device waist, and the inter-edges distance (IED) behind the Valsalva on a TEE plane including a short axis of the aorta and the device center (Fig. 3) at the phases when the device came nearest to the Valsalva and when the device went farthest from it in a cardiac cycle. When we recognized the Valsalva wall deformation pressed by either disc, we measured the maximum depth of the deformation from the standard curve of the Valsalva wall, as described in another study [6], and also confirmed what part of the disc was pressing the Valsalva wall, which was by the disc's edge or by the disc's inner plane, because pressure by the disc's edge is thought to be stronger than that by the disc's inner plane. Furthermore, we collected the information of complications that occurred until October 2020, such as device embolization, cardiac erosion, and atrioventricular block in the 47 patients.

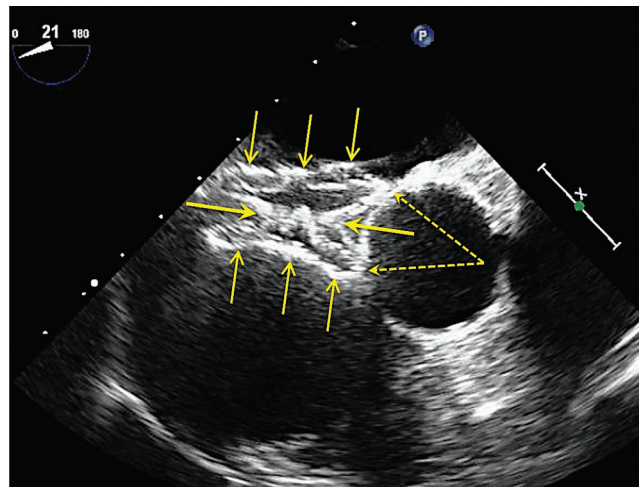


**Figure 3:** The waist and thickness of the device. We measured the device waist (between bold line arrows), maximum thickness at the center, Valsalva side, and the opposite side; these were on lines perpendicular to the line containing the device center, and the IED behind the aorta (between broken line arrows) on a TEE plane (containing the device's center and a short axis of the aorta)

#### 2.4 Study Procedure and Definition of Terms

1. We calculated a rate of successful procedure, which was defined when the device was not retrieved until the next day after placement.
2. We defined a device closure with no or small residual leakage as effective, which we evaluated by TEE at 6 months and by TTE at one year after the placement.

3. We clarified the onset and outcome of every serious complication during the follow-up period and calculated an incidence of them, respectively.
4. To evaluate device shape (especially behind the Valsalva), we calculated the flared index, defined as IED–(device thickness at the center). The index predicts how flared the device shapes over the Valsalva. Subsequently, we evaluated the relationship between device size–BSD and flared index at the nearest phases immediately and 6 months after placement, to investigate the relationship between device selection and flared shape. Furthermore, we evaluated the changes in device waist, device thicknesses, IED, and flared index over 6 months.
5. Concerning Valsalva wall deformation pressed by the discs, we summarized what part of the disc pressed the Valsalva wall and how deformed it became immediately and at 6 months after placement.

### 2.5 Statistical Analysis

We performed statistical analyses with Statcel 4 Software (OMS Publishing, Saitama, Japan). We presented continuous variables as mean  $\pm$  standard deviation or median and range appropriately. We used the paired *t*-test or Wilcoxon signed-rank test to compare the two groups. Moreover, we used the Pearson's correlation coefficient test to analyze the statistical relationship between two continuous variables. We considered *p*-values  $< 0.05$  as statistically significant.

### 3 Results

Tab. 1 shows baseline characteristics and TEE findings before placement in our study population. Most patients weighed above 20 kg in order to avoid conduction disorders. The mean maximum ASD diameter, BSD, device size, and device size–BSD were  $17.7 \pm 5.0$  mm,  $20.3 \pm 4.6$  mm,  $24.3 \pm 4.7$  mm, and  $4.0 \pm 1.6$  mm, respectively. Many patients (68.1%) had not only absent/extremely deficient aortic rim but also deficient superior rim. In the 47 patients, we recorded absent aortic rim in multiple views, bald aorta, and malaligned aortic/superior rim in 33, 30, and 18 patients, respectively.

**Table 1:** Patient characteristics and TEE findings before placement in 47 patients

		Mean $\pm$ standard deviation	Range
Age	[years]	$21.8 \pm 19.5$	6–73
Sex	Male: Female	16: 31	
Height	[cm]	$143 \pm 16$	113–171
Weight	[kg]	$38.5 \pm 15.3$	17.4–75.9
Body surface area	[m <sup>2</sup> ]	$1.23 \pm 0.10$	0.64–1.78
Qp/Qs		$2.28 \pm 0.77$	
Maximum ASD diameter	[mm]	$17.7 \pm 5.0$	8.8–29.8
BSD	[mm]	$20.3 \pm 4.6$	11.7–30.0
Device size	[mm]	$24.3 \pm 4.7$	15–33
Device size–BSD	[mm]	$4.0 \pm 1.6$	0.3–7.7
Minimum rim length			
Valsalva	[mm]	$0.2 \pm 0.4$	0–1.0
Superior	[mm]	$3.4 \pm 2.4$	0–8.0
Superior vena cava	[mm]	$6.3 \pm 2.9$	0–15.9
Posterior	[mm]	$11.0 \pm 5.5$	1.3–28.2

(Continued)

**Table 1 (continued).**

		Mean $\pm$ standard deviation	Range
Inferior vena cava	[mm]	13.0 $\pm$ 7.2	3.4–41.5
Coronary sinus	[mm]	13.3 $\pm$ 7.2	4.7–37.8
Mitral valve	[mm]	13.4 $\pm$ 5.5	7.3–24.8
Type of deficient rim			
Absent aortic rim in multiple views	[Number]	33/47 (70.2%)	
Bald aorta	[Number]	30/47 (63.8%)	
Malaligned aortic/superior rim	[Number]	18/47 (38.2%)	
Deficient superior rim	[Number]	32/47 (68.0%)	
Deficient posterior rim	[Number]	2/47	
Deficient inferior vena cava rim	[Number]	3/47	

All the 47 procedures were successful. [Tab. 2](#) displays data of each grade of residual leakage after placement. Although small leakage was recognized by TEE in 16 of 44 patients at 6 months after placement, leakage was not recognized by TTE one year after placement. We evaluated all device closures as effective at 6-month-follow-up time and after that, except in a patient who changed hospitals 3 months after placement. The mean observational period of these 46 patients was  $37.4 \pm 12.0$  months.

**Table 2:** Number of patients with residual leakage of each grade after device placement

Time	Leakage grade				Total number	Examination
	None	Small	Moderate	Large		
6 months later	28	16	0	0	44	TEE
1 year later	41	0	0	0	41	TTE
Latest follow-up time	46	0	0	0	46	TTE

Leakage grade with width of color Doppler: small  $\leq$  2 mm < moderate < 4 mm  $\leq$  large.

[Tab. 3](#) displays the pattern of complications after placement during the observation period. There were no serious complications. In one patient, we recognized a PR prolongation of 220 ms immediately after placement, which was spontaneously recovered 3 months later. In an 8-year-old boy having a maximum-25 mm ASD with absent aortic and superior rim, sinus node dysfunction with junctional rhythm occurred immediately after a 30 mm-device deployment. Pulling the connecting cable to move the right atrial disc off the septum immediately recovered sinus rhythm. Therefore, we sized down the device to 27 mm and maintained sinus rhythm thereafter. A BSD and an ASL were 25 mm and 34 mm. In another patient, we recognized a femoral arteriovenous fistula after placement that spontaneously closed up by the 2-year-follow-up time.

[Tab. 4](#) shows parameters about device shape and its change over 6 months. It demonstrates the data at phases when the device went farthest from the Valsalva and when it came nearest to it immediately and 6 months after placement. Immediately after placement, the device thickness and IED behind Valsalva at the nearest phase slightly increased than those at the farthest phase. These changes became smaller 6 months after placement. Although the device's thicknesses at center, Valsalva side, and opposite side significantly decreased by around 3.5 mm over 6 months, the IED did not change for 6 months. Thus, the flared index became larger over 6 months, though not significant.

**Table 3:** Complications after device placement in 47 patients

Complication	Number	Incidence (%)	Onset	Outcome
Death	0			
Device embolization	0			
Cardiac erosion	0			
Atrioventricular block (II°/III°)	0			
Atrioventricular block (I°)	1	2.1	Immediately after placement	Spontaneous recovery 3 months later
Sinus node dysfunction	1	2.1	Immediately after placement	Recovery by downsizing the device
Femoral arteriovenous fistula	1	2.1	Immediately after placement	Spontaneous closure within 2 years

**Table 4:** Device shape and its change over 6 months (n = 44)

Device shape		Immediately after placement		6 months after placement		Change in data over 6 months			
		Farthest phase	Nearest phase	Farthest phase	Nearest phase	Farthest phase	Nearest phase		
Waist	mm	19.0 ± 4.2	18.1 ± 4.3	17.6 ± 4.7	16.6 ± 4.9	-1.4	p < 0.001	-1.5	p < 0.001
Thickness									
Center (CT)	mm	12.1 ± 3.1	13.7 ± 3.6	8.7 ± 2.3	9.5 ± 2.6	-3.4	p = 0.005	-4.2	p = 0.001
Valsalva side	mm	18.0 ± 3.9	20.0 ± 4.5	14.6 ± 3.8	15.7 ± 4.0	-3.4	p < 0.001	-4.3	p < 0.001
Opposite side	mm	12.8 ± 2.8	14.1 ± 3.1	9.7 ± 2.0	10.6 ± 2.1	-3.1	p < 0.001	-3.5	p < 0.001
IED behind Valsalva sinus	mm	12.8 ± 2.6	14.5 ± 3.0	12.9 ± 3.2	13.9 ± 3.3	0.1	p = 0.70	-0.6	p = 0.79
Flared index (CT-IED)	mm	0.75 ± 3.2	0.84 ± 3.0	4.3 ± 2.4	4.5 ± 2.6	3.55	p = 0.99	3.66	p = 0.99

CT, center thickness; IED, inter-edges distance.

Fig. 4 shows the relationship between device selection and flared shape: (device size-BSD) and (Flared index at the nearest phase). The relationship between the two parameters is not recognized immediately after placement because the device tends to become bulky generally (Fig. 4A). However, the two have a positive correlation at 6 months after placement (n = 44, R = 0.32, p = 0.016) because the device thickness decreases, but the IED does not change over 6 months (Fig. 4B). These results indicate that the larger a selected device size was than the BSD, the more flared the device shapes behind the Valsalva over 6 months.

Tab. 5 summarizes the Valsalva wall deformation pressed by the discs, especially the point of impact and effect of deformation. We recognized a deformation in 13 of the 47 participants immediately after placement and in 28 of the 44 patients 6 months after placement. Although deformation was mostly due to pressure by either disc inner plane (Figs. 1F, 1I and Fig. 5D), it was due to pressure by the right atrial disc edge in one patient immediately after placement, and similar in another one 6 months after placement. In the former patient with absent and malaligned aortic rim, we selected a 27 mm FFII for a maximum 17.4 mm ASD diameter and a 22.0 mm BSD. Although the two disc edges behind the Valsalva shaped flared, they did not straddle enough over it. It was discovered later because the ratio of the Valsalva sinus diameter to the ASD diameter was larger than those in other patients. Therefore, the right atrial disc edge was intermittently pressing the Valsalva wall although the depth of deformation was only 1.0 mm immediately and 1.3 mm at 6 months after placement, respectively (Fig. 6). The depth of all these deformations was not so deep ranging from 0.5 mm–1.6 mm.

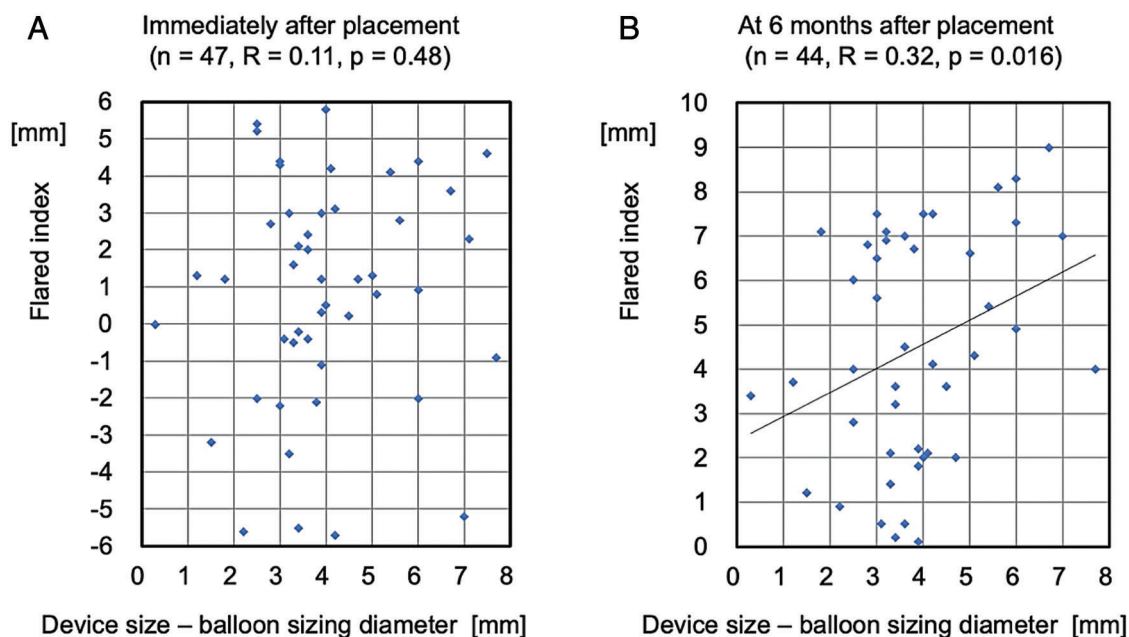


**Figure 4:** Relationship between (device size–balloon sizing diameter) and flared index

**Table 5:** Valsalva sinus wall deformation pressed by the discs in 47 patients

Valsalva wall deformation		Immediately after placement		6 months after placement	
		Left atrial disc	Right atrial disc	Left atrial disc	Right atrial disc
Number of patients	[n]	9/47	4/47	19/44	9/44
By disc inner plane	[n]	9	3	19	7
Depth of deformation	[mm]	1.2 (1.0–1.3)	1.0 (0.5–1.5)	1.2 (0.7–1.6)	1.0 (0.6–1.5)
By disc edge	[n]	0	1	0	2
Depth of deformation	[mm]		1.0		1.15 (1.0–1.3)

The data of depth of deformation are presented as median and range.

#### 4 Discussion

Selecting an appropriately sized device in ASD closure is often difficult because various problems (e.g., deficient rim in the aortic, superior, superior vena cava, posterior, inferior, coronary sinus, and/or mitral side; an aneurysmal/floppy rim; and short ASL) may exist. Hence, it is accompanied by serious complications (e.g., device embolization, erosion, or complete atrioventricular block), even though these incidences are rare [3–14]. Several technical skills have been used to avoid these serious complications, including balloon sizing by the stop-flow technique to avoid overstretching the defect, especially to avoid erosion [5], wiggling before detachment to ensure that the device is firmly deployed within the atrial septum [17], and selection of a device one size larger than would ordinarily be used in cases with a floppy rim to avoid device embolization [13].

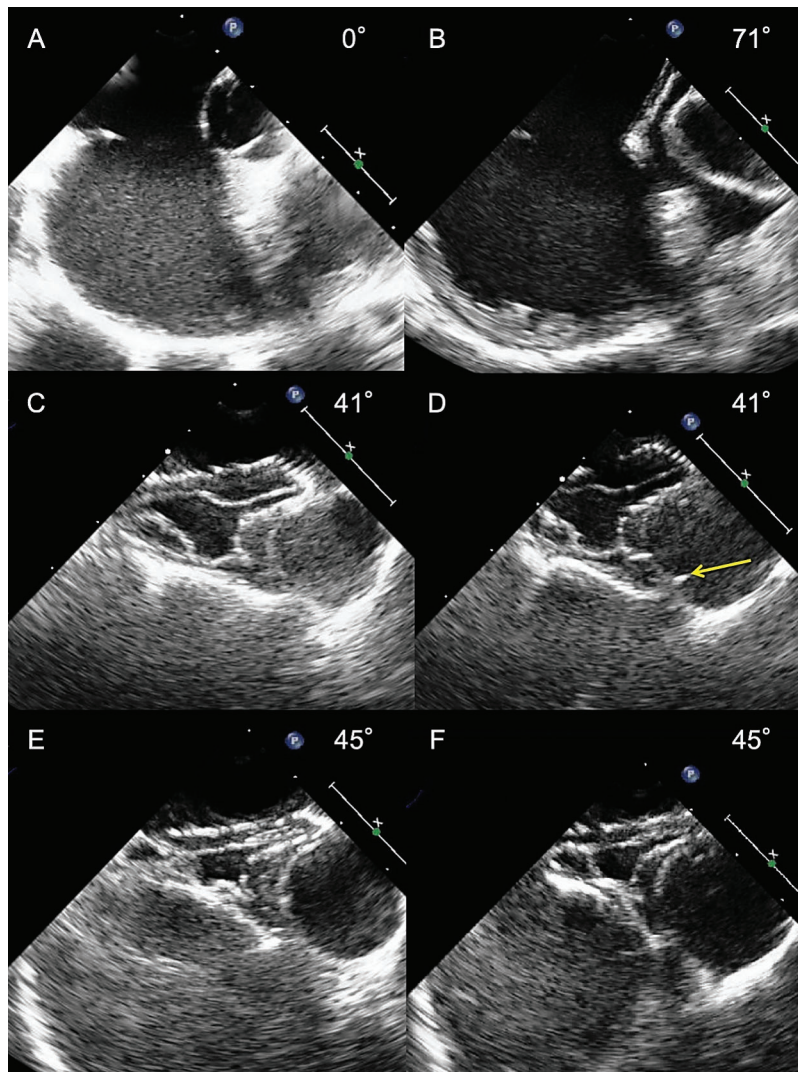


**Figure 5:** Transesophageal echocardiograms showing the inner plane of the disc pressing the Valsalva wall. A 30 mm FFII device was placed into the ASD for a BSD of 23.3 mm in an 8-year-old boy who had a 20 mm diameter ASD with an absent aortic rim in multiple views and bald aorta (A). Immediately after placement (C, the farthest phase of the device from the Valsalva; D, the nearest phase of the device), the whole device shape looks bulky, with two discs flared and straddling over the Valsalva and the inner plane of the right atrial disc slightly pressing the Valsalva wall intermittently, even though the maximum depth of the deformation is only 1.0 mm (D, arrow). At 6 months after placement (E, farthest phase; F, nearest phase), the whole device shape became compact, but the two discs became more flared over the Valsalva. Hence, the discs do not seem to be pressing the Valsalva wall

Our basic method of ASD device closure was as follows. Balloon sizing by TEE was performed to allow imaging of the device shape after placement on the surrounding structures and wiggling before detachment to make sure of the device's stability on the septum. Until June 2016, 908 and 30 patients were treated using an ASO and an FFII, respectively. Serious complications in the 938 patients included only aorta-right atrium fistula 3 months after placement in a patient. In the 938 patients, an ASO 0 mm–1 mm smaller than the BSD and an FFII 0 mm–2 mm larger than the BSD were usually selected. When wiggling migrated the

device off the septum, the device was replaced with a larger one (2 mm–3 mm). However, when the disc edge strongly pressed the aortic wall perpendicularly, the device was replaced with a smaller (1 mm–2 mm) or larger (2 mm–3 mm) one. When the disc edge of the upsized device still strongly pressed the aortic wall perpendicularly, it was further exchanged a larger one. In high-risk patients with an absent aortic rim or malaligned rim, TEE was routinely performed 6 months after placement to evaluate the device's shape, its changes, and disc's edge pressure on the aortic wall. After ASD placement, the shape of disc's edges behind the aorta often changes from flared to closed [6,15], which causes late onset cardiac erosion in the worst cases [6,8,9]. From these experiences, it was discovered that in some patients with an extremely deficient aortic rim undergoing placement of an FFII that was flared and straddling behind the aorta, the disc's edges did not press the aortic wall perpendicularly and the flared shape almost does not change for >6 months, and that a device 4 mm–6 mm larger than the BSD was finally selected. Then, this method was considered to intentionally make the FFII flared and straddling behind the aorta to avoid device embolization and erosion, especially in cases with absent aortic rim or malaligned rim.

This study sought to clarify the midterm efficacy and safety of ASD closure in patients with absent and/or malaligned aortic and/or superior rim using FFII devices flared and straddling behind the aorta. Such device shape is thought to avoid device embolization as well as cardiac erosion if the shape is kept for a long time. Actually, such device shape was made by selecting a FFII device 4 to 6-mm larger than the BSD by stop-flow technique in most patients. ASD closure with this method is evaluated as effective because all the 47 procedures were successful, and residual leakage disappeared by 1 year after placement in all the patients who were followed up. Also, this method is considered as safe because complications in the 46 patients for a mean observation period of  $37 \pm 12$  months included only first-degree atrioventricular block within 3 months in one patient and femoral arteriovenous fistula in another one. However, there is a possibility that this method has a serious conduction disorder such as complete atrioventricular block or sinus node dysfunction because of selecting a larger size device than the BSD. Actually, we recognized a transient sinus node dysfunction immediately after device placement in one patient although recovery of sinus rhythm occurred immediately after downsizing the device. According to a report including more than 1300 patients after Occlutech devices placement, transient atrioventricular block occurred in 7 patients with recovery in 5 of them, while new onset atrioventricular block occurred in 3 patients, 1 of whom had an oversized device implanted and removed surgically [11]. Therefore, we should avoid selecting excessively large device, especially in small children around 20 kg or less whose cardiac structures are not strong. In small children with absent or extremely deficient aortic rim and short ASL, selection of the largest device, the diameter of which plus the rim length of left atrial disc is no more than the BSD plus 2 mm, usually makes the two discs flared and straddled behind the Valsalva without serious conduction disorders.

Concerning device shape and change over time, when a FFII 4 to 6-mm larger than the BSD is placed into the ASD with absent and/or malaligned aortic and/or superior rim, the device tends to be shaped bulky generally, flared and straddling behind the Valsalva immediately after placement. This is possibly because the right atrial disc edge turns outward from the connecting waist plane while the left atrial disc is flexible to change the shape. From results of the study, the device loses this flexibility and becomes more compact similar to ASO, but the two discs remain flared and straddling behind the aorta over 6 months unlike ASO [15]. Hence, if any disc presses the Valsalva wall, there is very unlikely that cardiac erosion will occur because the pressure is usually by the disc inner plane.

Cases of erosion after FFII placement were reported less compared with those of ASO [2,4,11,14]. One reason is probably that the FFII design of the left disc has no hub and contains less metal in the center to provide better flexibility and less impingement of the aortic vessel walls if placed adjacent to them [11]. However, this study revealed that FFII almost loses flexibility >6 months. From previous reports, slightly larger devices for BSD seemed to be placed in patients undergoing FFII placement than in those undergoing ASO placement. In more than 1300 cases after FFII placement, the mean BSD/device size was

18.1 mm/20.5 mm [11], whereas that in 125 cases developing erosion after ASO placement was 21.2 mm/22.6 mm and in 250 control cases without erosion was 19.0 mm/20.3 mm [4]. In the 125 erosion cases, the ratio of oversized devices was <25% after balloon sizing by the stop-flow technique, as recommended in 2004 [5]. Also, an oversized device was placed in only one of the seven erosion cases after FFII placement [14]. Furthermore, in 12 erosion cases with an appropriately sized ASO placement, either disc edge strongly pressed the aortic wall perpendicularly in most cases, those were also confirmed at the surgical corrections [6]. Thus, the pressure of a disc edge on the aortic wall is thought to be a bigger problem than an oversized device [6,7]. It is considered that a combination of sustained flexibility of the left atrial disc for several months [11] and the two discs been flared and straddling over the aorta decrease the incidence of erosion in patients undergoing FFII placement compared to ASO placement.

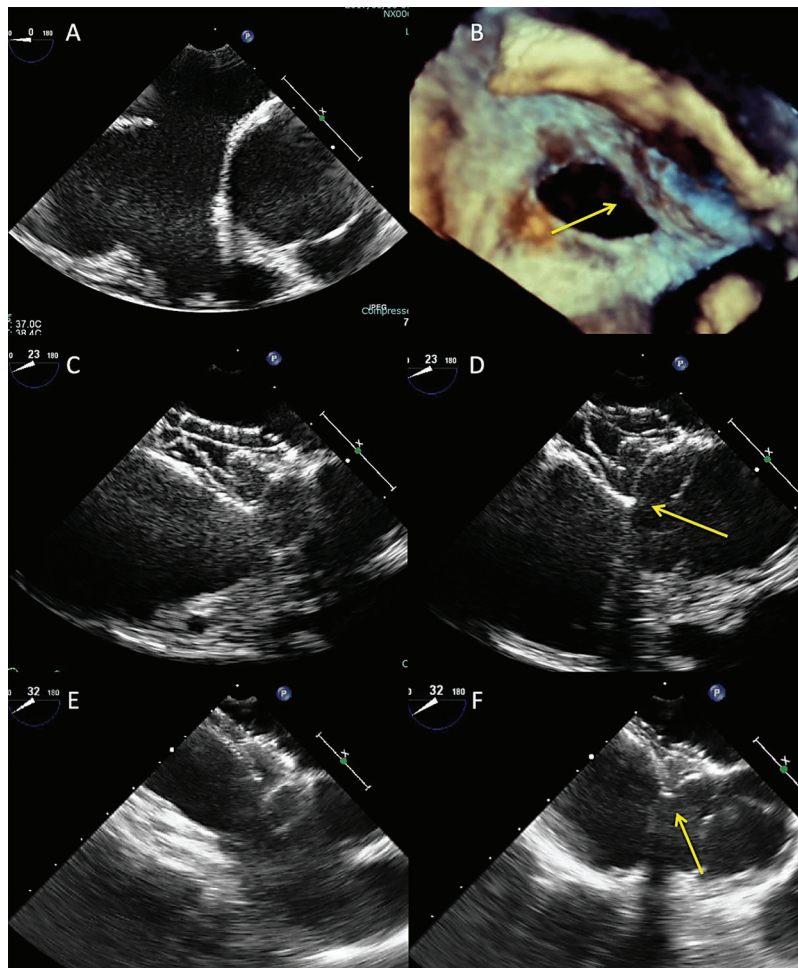


**Figure 6:** Transesophageal echocardiograms showing the disc edge perpendicularly pressing the Valsalva wall. A 45-year-old female had a 17.4 mm diameter ASD with absent aortic rim in multiple views, bald aorta, and malaligned aortic rim (A, B, arrow). A 27 mm FFII device was placed into the ASD for a 22 mm BSD. Immediately after placement (C, the farthest phase of the device from the Valsalva, D, the nearest phase of the device), the two discs flared but were not straddling enough over the Valsalva. Hence, the right atrial disc edge is perpendicularly pressing the Valsalva wall intermittently, even though the maximum depth of the deformation is only 1.0 mm (D, arrow). At 6 months after placement (E, farthest phase; F, nearest phase), the whole device becomes compact, the two discs remain flared without straddling enough over the Valsalva and the right atrial disc edge is still intermittently pressing the Valsalva wall, even though the maximum depth of the deformation is only 1.3 mm (F, arrow)

When closing an ASD with a widely malaligned aortic/superior rim, we have to pay attention especially to a patient with a very large Valsalva relative to ASD. Such an ASD requires selection of a much larger device to shape straddling over the aorta. We treated such an ASD patient with malaligned absent aortic and superior rim as follows. For a  $9.2 \text{ mm} \times 7.3 \text{ mm}$  ASD, we placed a 21 mm FFII around 8 mm larger than the BSD. The device was shaped flared behind the aorta as well as bulky generally, thereby straddling over the aorta. At 6-month-follow-up time, TEE showed that the whole device shape became slightly compact, but the two discs were flared and straddling over the aorta (Fig. 7).

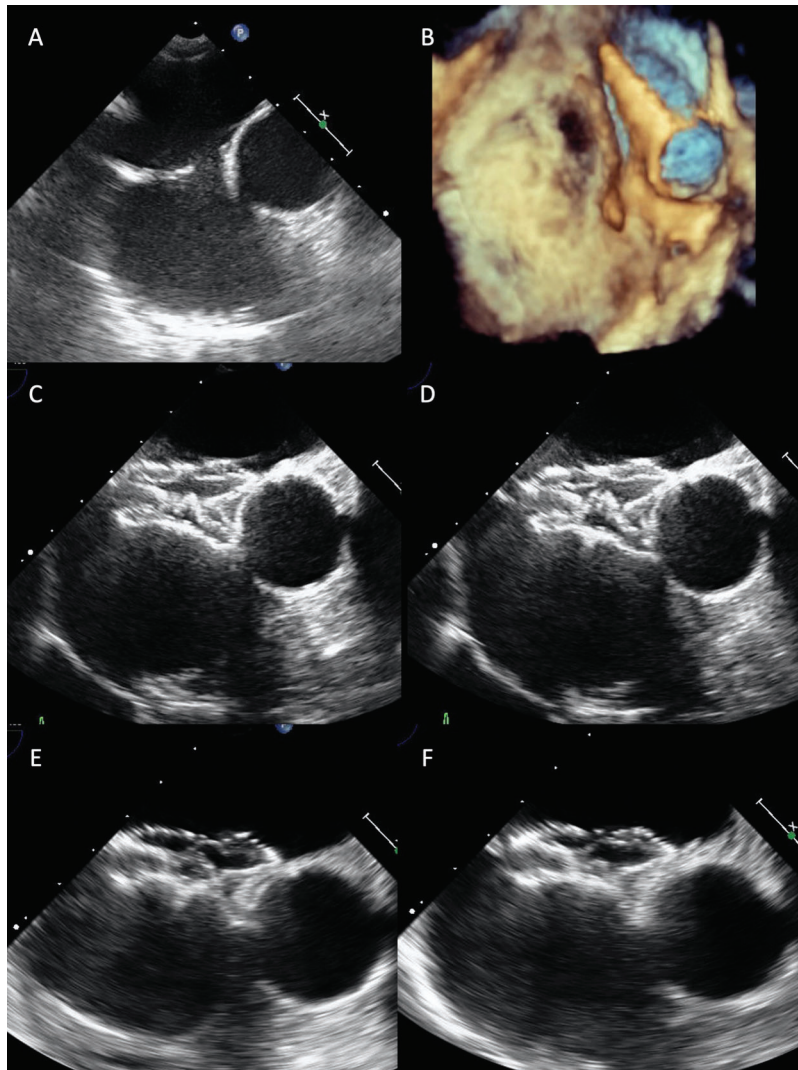


**Figure 7:** Transesophageal echocardiograms revealing how to close a small ASD relative to the large aorta with a malaligned absent rim. A 21 mm FFII device was placed into the ASD for a 13 mm BSD in a 68-year-old patient who had a  $9.2 \text{ mm} \times 5.2 \text{ mm}$  diameter small ASD relative to the large aorta with widely malaligned absent aortic and superior rim (A, B). Immediately after placement (C, the farthest phase of the device from the aorta; D, the nearest phase of the device), two discs flare and the whole device shape becomes bulky, thus straddling over the aorta without pressure to the aortic wall. At 6 months after placement (E, farthest phase; F, nearest phase), the whole device shape becomes slightly compact, but the two discs become more flared over the aorta. Hence, the disc edges do not appear to be pressing the aortic wall

## 5 Limitations

The small sample size coupled with the single-center nature of the study makes it not externally validated. We therefore recommend a large sample-sized multicenter study be performed in future.

## 6 Conclusion

Midterm outcome of ASD closure using a FFII device shaped flared and straddling over the aorta is considered effective and safe for patients with absent and/or malaligned aortic and/or superior rim although the long-term outcome is not clear. This method probably avoids device migration as well as cardiac erosion; although it requires great care for serious conduction disorders especially in small children with short ASL.

**Data Sharing:** Data are available on reasonable request.

**Funding Statement:** The authors received no specific funding for this study.

**Conflicts of Interest:** The authors declare that they have no conflicts of interest to report regarding the present study.

## References

1. Du, Z. D., Hijazi, Z. M., Kleinman, C. S., Silverman, N. H., Larntz, K. et al. (2002). Comparison between transcatheter and surgical closure of secundum atrial septal defect in children and adults: Results of a multicentre nonrandomized trial. *Journal of the American College of Cardiology*, 39(11), 1836–1844. DOI 10.1016/S0735-1097(02)01862-4.
2. DiBardino, D. J., McElhinney, D. B., Kaza, A. K., Mayer, J. E. Jr. (2009). Analysis of the US Food and Drug Administration Manufacturer and User Facility Device Experience database for adverse events involving Amplatzer septal occluder devices and comparison with the Society of Thoracic Surgery congenital cardiac surgery database. *Journal of Thoracic and Cardiovascular Surgery*, 137(6), 1334–1341. DOI 10.1016/j.jtcvs.2009.02.032.
3. Levi, D. S., Moore, J. W. (2004). Embolization and retrieval of the Amplatzer septal occluder. *Catheterization and Cardiovascular Interventions: Official Journal of the Society for Cardiac Angiography & Interventions*, 61(4), 543–547. DOI 10.1002/ccd.20011.
4. McElhinney, D. B., Quartermain, M. D., Kenny, D., Alboliras, E., Amin, Z. (2016). Relative risk factors for cardiac erosion following transcatheter closure of atrial septal defects: A case-control study. *Circulation*, 133(18), 1738–1746. DOI 10.1161/CIRCULATIONAHA.115.019987.
5. Amin, Z., Hijazi, Z. M., Bass, J. L., Cheatham, J. P., Hellenbrand, W. E. et al. (2004). Erosion of Amplatzer septal occluder device after closure of secundum atrial septal defects: Review of registry of complications and recommendations to minimize future risk. *Catheterization and Cardiovascular Interventions: Official Journal of the Society for Cardiac Angiography & Interventions*, 63(4), 496–502. DOI 10.1002/ccd.20211.
6. Kitano, M., Yazaki, S., Sugiyama, H., Ohtsuki, S. I., Tomita, H. (2020). Risk factors and predictors of cardiac erosion discovered from 12 Japanese patients who developed erosion after atrial septal defect closure using Amplatzer septal occluder. *Pediatric Cardiology*, 41(2), 297–308. DOI 10.1007/s00246-019-02256-3.
7. El-Said, H. G., Moore, J. W. (2009). Erosion by the Amplatzer septal occluder: Experienced operator opinions at odds with manufacturer recommendations? *Catheterization and Cardiovascular Interventions: Official Journal of the Society for Cardiac Angiography & Interventions*, 73(7), 925–930. DOI 10.1002/ccd.21931.
8. Chun, D. S., Turrentine, M. W., Moustapha, A., Hoyer, M. H. (2003). Development of aorta-to-right atrial fistula following closure of secundum atrial septal defect using the Amplatzer septal occluder. *Catheterization and cardiovascular interventions: Official journal of the Society for Cardiac Angiography & Interventions*, 58(2), 246–251. DOI 10.1002/ccd.10434.

9. Jang, G. Y., Lee, J. Y., Kim, S. J., Shim, W. S., Lee, C. H. (2005). Aorta to right atrial fistula following transcatheter closure of an atrial septal defect. *American Journal of Cardiology*, 96(11), 1605–1606. DOI 10.1016/j.amjcard.2005.08.012.
10. Amin, Z. (2014). Echocardiographic predictors of cardiac erosion after Amplatzer septal occluder placement. *Catheterization and Cardiovascular Interventions*, 83(1), 84–92. DOI 10.1002/ccd.25175.
11. Haas, N. A., Soetemann, D. B., Ates, I., Baspinar, O., Ditskivskyy, I. et al. (2016). Closure of secundum atrial septal defects by using the Occlutech occluder devices in more than 1300 patients: The IRFACODE project: A retrospective case series. *Catheterization and Cardiovascular Interventions: Official Journal of the Society for Cardiac Angiography & Interventions*, 88(4), 571–581. DOI 10.1002/ccd.26497.
12. Abe, T., Tsukano, S., Tosaka, Y. (2019). Pericardial tamponade due to erosion of a Figulla Flex II device after closure of an atrial septal defect. *Catheterization and Cardiovascular Interventions: Official Journal of the Society for Cardiac Angiography & Interventions*, 94(7), 1003–1005. DOI 10.1002/ccd.28367.
13. Roymanee, S., Promphan, W., Tonklang, N., Wongwaitaweewong, K. (2015). Comparison of the Occlutech® Figulla® septal occluder and Amplatzer® septal occluder for atrial septal defect device closure. *Pediatric Cardiology*, 36(5), 935–941. DOI 10.1007/s00246-015-1103-y.
14. Auriiau, J., Bouvaist, H., Aaberge, L., Abe, T., Dähnert, I. et al. (2019). Cardiac erosions after transcatheter atrial septal defect closure with the Occlutech Figulla Flex device. *JACC: Cardiovascular Interventions*, 12(14), 1397–1399. DOI 10.1016/j.jcin.2019.03.005.
15. Kitano, M., Yazaki, S., Sugiyama, H., Yamada, O. (2009). The influence of morphological changes in amplatzer device on the atrial and aortic walls following transcatheter closure of atrial septal defects. *Journal of Interventional Cardiology*, 22(1), 83–91. DOI 10.1111/j.1540-8183.2008.00421.x.
16. Kenny, D., Eicken, A., Dähnert, I., Boudjemline, Y., Sievert, H. et al. (2019). A randomized, controlled, multi-centre trial of the efficacy and safety of the Occlutech Figulla Flex-II Occluder compared to the Amplatzer Septal Occluder for transcatheter closure of secundum atrial septal defects. *Catheterization and Cardiovascular Interventions*, 93(2), 316–321. DOI 10.1002/ccd.27899.
17. Berger, F., Ewert, P., Dähnert, I., Stiller, B., Nürnberg, J. H. et al. (2000). Interventional occlusion of atrial septum defects larger than 20 mm in diameter. *Z Kardiologie*, 89(12), 1119–1125. DOI 10.1007/s003920070139.